

# Estimating gluconeogenesis by NMR isotopomer distribution analysis of [ $^{13}\text{C}$ ]bicarbonate and [ $1\text{-}^{13}\text{C}$ ]lactate

Tiago Cardoso Alves,<sup>1</sup> Patrícia Maria Nunes,<sup>2</sup> Carlos Marques Palmeira,<sup>2</sup>  
John Griffith Jones<sup>2</sup> and Rui Albuquerque Carvalho<sup>1\*</sup>

<sup>1</sup>Department of Biochemistry, Faculty of Sciences and Technology, University of Coimbra, Coimbra, Portugal

<sup>2</sup>Center for Neurosciences and Cellular Biology of Coimbra, Department of Zoology, University of Coimbra, Coimbra, Portugal

Received 20 October 2006; Revised 19 April 2007; Accepted 31 May 2007

**ABSTRACT:** The gluconeogenic contribution to glucose production in livers isolated from rats fasted for 24 h was determined by  $^{13}\text{C}$ -NMR isotopomer distribution analysis of secreted glucose enriched from 99% [ $^{13}\text{C}$ ]bicarbonate ( $n = 4$ ) and 99% [ $1\text{-}^{13}\text{C}$ ]lactate ( $n = 4$ ). Experiments with 3%  $^2\text{H}_2\text{O}$  were also performed, allowing the gluconeogenic contribution to be measured by the relative  $^2\text{H}$  enrichments at positions 5 and 2 of glucose. From  $^{13}\text{C}$ -NMR analyses, the contribution of gluconeogenesis to glucose output was estimated to be  $93 \pm 3\%$  for [ $^{13}\text{C}$ ]bicarbonate perfusion and  $91 \pm 3\%$  for [ $1\text{-}^{13}\text{C}$ ]lactate perfusion, in good agreement with the  $^2\text{H}$ -NMR analysis of the gluconeogenic contribution to glucose production ( $100 \pm 1\%$  and  $99 \pm 1\%$ , respectively) and consistent with the expected negligible contribution from glycogenolysis. These results indicate that  $^{13}\text{C}$ -NMR analysis of glucose  $^{13}\text{C}$ -isotopomer distribution from either [ $^{13}\text{C}$ ]bicarbonate or [ $1\text{-}^{13}\text{C}$ ]lactate precursor provides realistic estimates of the gluconeogenic contribution to hepatic glucose output. Copyright © 2007 John Wiley & Sons, Ltd.

**KEYWORDS:** gluconeogenesis; glucose production; NMR isotopomer distribution analysis; liver

## INTRODUCTION

During fasting, hepatic glucose is produced by glycogen hydrolysis and gluconeogenesis (GNG). Rates of hepatic glucose synthesis from these sources are influenced by nutritional, hormonal and disease states. Therefore, measurement of these fluxes provides key insights into relationships between glucose metabolism and whole-body physiology and pathophysiology. Traditionally, GNG has been measured by comparing the enrichment or specific radioactivity of a representative precursor substrate, such as alanine or lactate, with that of plasma glucose after infusion of  $^{13}\text{C}$ - or  $^{14}\text{C}$ -labeled alanine or lactate tracer. However, with this approach, three factors reduce the precision of the measurement: (1) true hepatic precursor enrichment is difficult to measure *in situ*; (2) there is unspecified loss and dilution of the tracer by exchange with Krebs cycle intermediates; (3) the contributions of glycerol GNG and glycogenolysis to

glucose production (GP) cannot be resolved, as both processes dilute the  $^{13}\text{C}$  enrichment or  $^{14}\text{C}$  specific radioactivity of plasma glucose relative to that of the precursor pool. Mass isotopomer distribution analysis (MIDA) overcomes these limitations by relating the tracer enrichment of plasma glucose to that of the immediate triose phosphate precursors (1,2). As any dilution of the tracer between triose phosphate and glucose can only arise from unlabeled glucose generated by glycogenolysis, the method provides a measurement of the total GNG contribution to GP relative to glycogenolysis. The measurement is also practical in that enrichment of triose phosphate precursor is calculated from the isotopomer distribution of plasma glucose, eliminating the need to measure the enrichment of hepatic precursor pools. A key assumption of MIDA is that the tracer has equal access to all hepatic GNG activity. One of the conditions is that the tracer arteriovenous concentration gradient across the hepatic lobule must be relatively small so that periportal and perivenous hepatocytes have equal access to the tracer. This applies for some substrates such as lactate, but not for other GNG precursors that are quantitatively extracted from the circulation by the liver, such as glycerol (3,4). The resulting concentration gradient of glycerol across the hepatic lobule means that periportal cells experience higher tracer concentrations than perivenous cells. Consequently, the [ $^{13}\text{C}$ ]isotopomer distribution of glucose obtained from [ $^{13}\text{C}$ ]glycerol is

\*Correspondence to: R. A. Carvalho, Department of Biochemistry, Apartado 3126, 3001-401 Coimbra, Portugal.  
E-mail: carvalho@ci.uc.pt

Contract/grant sponsor: FCT-MCES; contract/grant numbers: POCTI/CBO/38611/01, POCTI/QUI/55603/2004 and POCI/SAU-OBS/55802/04.

**Abbreviations used:** GNG, gluconeogenesis; GP, glucose production; MAG, monoacetone derivative of glucose; MIDA, mass isotopomer distribution analysis; NA, natural abundance; PEP, phosphoenolpyruvate.

weighted towards the relatively high local enrichment of the periportal triose phosphate pool. This leads to an overestimate of hepatic triose phosphate  $^{13}\text{C}$  enrichment and a corresponding underestimation of the fraction of GP derived from GNG. Thus, under starvation conditions in which hepatic glycogen is depleted and GNG is expected to contribute  $\sim 100\%$  of GP, MIDA with either  $[2-^{13}\text{C}]$  glycerol or  $[\text{U-}^{13}\text{C}]$  glycerol gave improbably low estimates of the GNG fraction (5). To date, there have been no reported studies of alternative GNG tracers that are more evenly distributed across the hepatic lobule and might therefore provide more valid estimates of GNG by MIDA.

We reasoned that  $[^{13}\text{C}]$  bicarbonate might be an effective tracer for quantification of GNG by isotopomer distribution analysis because its hepatic arteriovenous concentration gradient is small and its concentration is not a limiting factor for carboxylation reactions anywhere in the liver. As with  $[^{14}\text{C}]$  bicarbonate (6), incorporation of  $[^{13}\text{C}]$  bicarbonate into glucose requires the carboxylation of an anaplerotic substrate such as pyruvate to form  $[1-^{13}\text{C}]$  oxaloacetate. Exchange of oxaloacetate with malate and fumarate results in an approximately equal distribution of  $^{13}\text{C}$  enrichment in  $[1-^{13}\text{C}]$  oxaloacetate and  $[4-^{13}\text{C}]$  oxaloacetate. GNG utilization of  $[4-^{13}\text{C}]$  oxaloacetate via phosphoenolpyruvate carboxykinase results in the formation of  $[1-^{13}\text{C}]$  phosphoenolpyruvate (PEP) and subsequent  $[1-^{13}\text{C}]$  triose phosphates. Glucose is formed from two triose phosphate units, and the probability of generating  $[3,4-^{13}\text{C}_2]$  glucose is a function of the enrichment of the precursor  $[1-^{13}\text{C}]$  triose phosphate (Fig. 1).

The glucose isotopomer populations can be quantified directly by  $^{13}\text{C}$ -NMR spectroscopy because  $[3,4-^{13}\text{C}_2]$  glucose generates doublet signals as a result of  $^{13}\text{C}$ - $^{13}\text{C}$  coupling that are resolved from the singlet resonances of  $[3-^{13}\text{C}]$  glucose and  $[4-^{13}\text{C}]$  glucose. The fractional enrichment of the triose phosphate precursor pool is directly obtained from the ratio of the doublet to singlet signals, as shown in Fig. 1. As only C3 and C4 of glucose are enriched from  $[^{13}\text{C}]$  bicarbonate, the other  $^{13}\text{C}$  signals of glucose represent background natural abundance (NA) at 1.1%, and, as such, they provide convenient internal standards for estimating excess  $^{13}\text{C}$  enrichment in C3 and C4 of glucose. Thus, by comparing the actual glucose enrichment with that of the triose phosphate precursor derived by isotopomer distribution analysis, the fraction of glucose derived from triose phosphate (assumed to be equal to the fraction derived by GNG) can be estimated. [Glycogen conversion into glucose is assumed to occur entirely via the direct pathway (glycogen  $\rightarrow$  Glc1P  $\rightarrow$  Glc6P  $\rightarrow$  glucose). Any glycogen that is converted into C3 compounds before Glc6P and glucose will be counted as GNG.]  $[1-^{13}\text{C}]$  Lactate is converted into  $[4-^{13}\text{C}]$  oxaloacetate via lactate dehydrogenase and pyruvate carboxylase, therefore it provides the same gluconeogenic precursor enrichment pattern as  $[^{13}\text{C}]$  bicarbonate.

In this report, we show that estimates of  $[1-^{13}\text{C}]$  triose precursor enrichment using the isotopomer distribution analysis of Neese *et al.* (2) can be simply and directly obtained by  $^{13}\text{C}$ -NMR spectroscopy of the monoacetone derivative of glucose (MAG), as shown schematically in

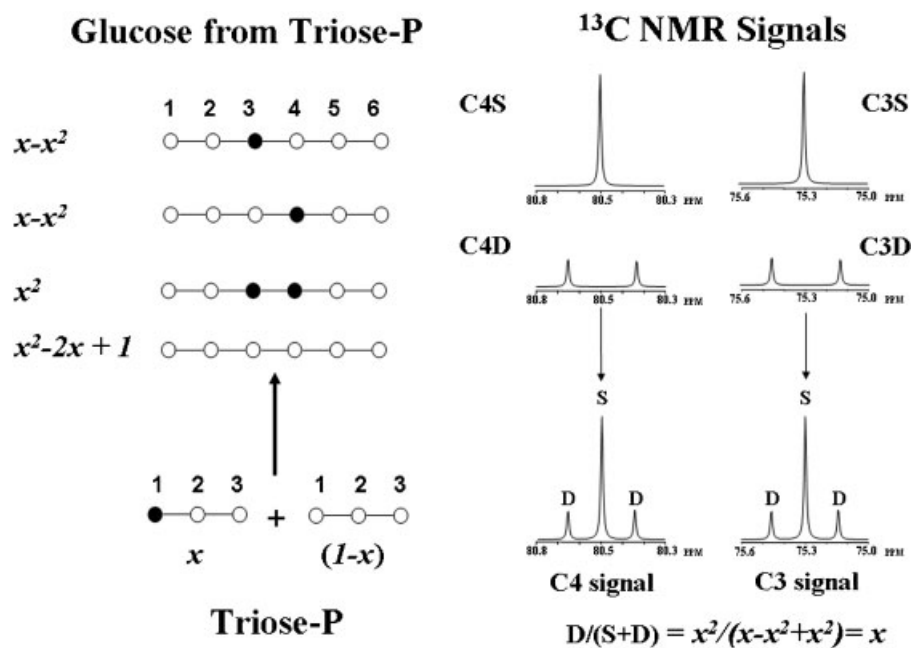


**Figure 1.** Glucose  $^{13}\text{C}$  isotopomer distribution from triose phosphate (Triose-P) and corresponding simulated NMR spectrum. Glucose labeled in only one position (C3 or C4) is represented by a single signal (S) in the NMR spectrum. Glucose labeled in both carbons produces a doublet signal (D) because of the  $^{13}\text{C}3-^{13}\text{C}4$  coupling. The symbol  $x$  represents the probability of the pool of triose phosphate being labeled with  $^{13}\text{C}$  in C1.

Fig. 1. To determine if this approach provides realistic estimates of the GNG contribution to GP, we applied the method to perfused livers obtained from rats fasted for 24 h, in which the contribution of GNG to GP is expected to approach 100%. We compared this method with the  $^2\text{H}_2\text{O}$  measurement of fractional GNG based on the  $^2\text{H}$ -enrichment ratio in positions 5 and 2 of glucose (H5/H2). In either perfused or *in situ* livers depleted of glycogen, the H5/H2 ratio provides realistic estimates of the fraction of GP derived from GNG (i.e. approaching 100% contribution). This ratio can be derived by  $^2\text{H}$ -NMR spectroscopy of the MAG derivative without interference from the  $^{13}\text{C}$ -enrichment distributions (7–11). Likewise, the [ $^{13}\text{C}$ ]isotopomer analysis is not modified by the presence of 2–3%  $^2\text{H}$  enrichment, therefore the deuterated water and  $^{13}\text{C}$ -labeled tracer can be administered at the same time.

## MATERIALS AND METHODS

### Materials

$^{13}\text{C}$ -enriched compounds (sodium [ $^{13}\text{C}$ ]bicarbonate and sodium [1- $^{13}\text{C}$ ]lactate) and  $^2\text{H}_2\text{O}$  were purchased from Cambridge Isotope Laboratories (Cambridge, MA, USA) and Eurisotop (Saint-Aubin, France), respectively. Other materials were analytical grade and used without further purification (Sigma, St Louis, MO, USA).

### Experimental design

Healthy male Wistar Han rats, 12 weeks old, were purchased from Charles River Laboratories, Barcelona, Spain. After being starved for 24 h, the animals were randomly divided into two groups. Before liver removal, each animal was anesthetized with an intraperitoneal injection of ketamine (200  $\mu\text{L}/100\text{ g}$  body weight). Then, with the portal vein cannulated, each liver was perfused ( $>20\text{ mL}/\text{min}$  for 10 min) with Krebs-Henseleit bicarbonate/ $\text{H}_2\text{O}$  buffer bubbled continuously with a 95%/5% mixture of  $\text{O}_2/\text{CO}_2$  at  $37^\circ\text{C}$ . After this wash-out period, the livers of one group were perfused ( $>20\text{ mL}/\text{min}$  for 20 min) with Krebs-Henseleit [ $^{13}\text{C}$ ]bicarbonate/3%  $^2\text{H}_2\text{O}$  buffer supplemented with 1.0 mM lactate, 0.1 mM pyruvate and 0.2 mM octanoate, and the livers of the second group were perfused with Krebs-Henseleit bicarbonate/3%  $^2\text{H}_2\text{O}$  buffer supplemented with 1.0 mM [1- $^{13}\text{C}$ ]lactate, 0.1 mM pyruvate and 0.2 mM octanoate.

The perfusates obtained were lyophilized, and all the glucose present in the extracts was converted into MAG as described by Snowden (12). The lyophilized extracts were treated with excess anhydrous deuterated acetone and concentrated  $\text{H}_2\text{SO}_4$  (4%, v/v) and stirred for 4 h. Water was then added to the reaction mixture, and the sample was neutralized with 2 M NaOH. The pH was then

adjusted to 2.0 with dilute HCl, and the solution was kept for 5 h at  $40^\circ\text{C}$ . The reaction was stopped by elevating the pH to 8–9 with 2 M NaOH, and the solvent was removed by rotary evaporation. MAG was extracted from the dried residue with a few milliliters of boiling ethyl acetate, and the residue of the new extraction was dissolved in 600  $\mu\text{L}$  90% acetonitrile/10% water.

### NMR analysis

NMR spectra were acquired using a 5 mm broadband probe on a 11.7 T Varian Unity spectrometer (Varian Instruments, Palo Alto, CA, USA) at  $50^\circ\text{C}$ . Proton-decoupled  $^{13}\text{C}$ -NMR spectra of liver and perfusate samples were acquired using a  $45^\circ$  pulse, a 1.5 s acquisition time, and an interpulse delay of 3 s. Proton-decoupled  $^2\text{H}$  NMR spectra of the perfusate samples were obtained in the unlocked mode using a  $90^\circ$  pulse, a 1.5 s acquisition time, and no interpulse delay. Deconvolution and quantification of  $^{13}\text{C}$  and  $^2\text{H}$  NMR signals were performed with the curve-fitting routine supplied with the NUTS<sup>TM</sup> PC-based NMR spectral analysis program (Acorn NMR, Inc., Fremont, CA, USA).

### Contribution of GNG to hepatic GP by isotopomer distribution analysis of glucose enrichment from $^{13}\text{C}$ -labeled tracers

The percentage  $^{13}\text{C}$  enrichment of glucose in C3 and C4 (Glc3F, Glc4F) was determined by the ratio of the total C3 or C4 signal relative to the neighboring NA C2 or C5 signals multiplied by 100. Excess  $^{13}\text{C}$  enrichment in C3 and C4 was determined by subtracting 1.1% from Glc3F and Glc4F.

Triose phosphate precursor enrichment,  $x_n$ , was estimated from the C3 multiplet ( $x_3$ ) and C4 ( $x_4$ ) multiplet by the following equations:

$$x_3 = \text{C3D34}/(\text{C3S} + \text{C3D34}) \quad (1)$$

$$x_4 = \text{C4D34}/(\text{C4S} + \text{C4D34}) \quad (2)$$

where C3S and C4S are the relative areas of the C3 and C4 singlet signals after subtraction of NA contributions, and C3D34 and C4D34 are the relative areas of the C3 and C4 doublet signals.

The percentage of glucose derived from GNG was calculated from the triose phosphate and glucose enrichments of C3 and C4 as follows:

Percentage glucose from GNG, C3 analysis

$$= 100 \times \text{Glc3F}/x_3 \quad (3)$$

Percentage glucose from GNG, C4 analysis

$$= 100 \times \text{Glc4F}/x_4 \quad (4)$$

From the  $^2\text{H}$  NMR spectra of MAG, the percentage contribution of glycogenolysis and GNG was evaluated by the ratio of deuterium signal intensities of positions 2 and 5 according to the following equation [7]:

$$\text{Glycogenolysis contribution to GP :} \\ [1 - (\text{signal 5/signal 2})] \times 100 \quad (5)$$

$$\text{GNG contribution to GP :} \\ (\text{signal 5/signal 2}) \times 100 \quad (6)$$

## Data presentation and statistical analysis

The results are presented as mean  $\pm$  SE. A statistical analysis was performed using the Mann-Whitney U test, a non-parametric alternative to the  $t$  test for independent samples. In this test, two populations are considered statistically different if  $U_{\text{calc}} \geq U_{\text{table}}$ .

## RESULTS

### Glucose enrichment from $[^{13}\text{C}]$ bicarbonate and $[1-^{13}\text{C}]$ lactate assessed by $^{13}\text{C}$ NMR

The MAG derivative generates narrow and well-resolved  $^{13}\text{C}$ -NMR signals for all hexose carbons (10,13,14). Representative  $^{13}\text{C}$ -NMR spectra derived from the  $[^{13}\text{C}]$ bicarbonate/ $^2\text{H}_2\text{O}$  and  $[1-^{13}\text{C}]$ lactate/ $^2\text{H}_2\text{O}$  labeling experiments are represented in Fig. 2. As expected, the two spectra are very similar as, with both tracers, position 1 of PEP and positions 3 and 4 of glucose are enriched with  $^{13}\text{C}$ . In addition, the  $^{13}\text{C}$ -NMR signals are not significantly perturbed by the low  $^2\text{H}$ -enrichment level of glucose ( $\leq 3\%$ ). (Substitution of  $^1\text{H}$  by  $^2\text{H}$  results in additional splitting of directly bound  $^{13}\text{C}$  via  $^{13}\text{C}$ – $^2\text{H}$  coupling as well as an isotope shift for both directly bound and neighboring  $^{13}\text{C}$  nuclei. With methine functionalities, the directly bound  $^{13}\text{C}$  has no nuclear Overhauser enhancement and its  $T_1$  is increased.) The signals of C1, C2, C5 and C6 are derived from NA  $^{13}\text{C}$  and represent 1.1% enrichment. The signals of C3 and C4 are more intense and reflect enrichment from the GNG incorporation of  $[^{13}\text{C}]$ bicarbonate. The total  $^{13}\text{C}$  enrichment of C3 tended to be higher than that of C4 (Table 1), indicating that  $^{13}\text{C}$  enrichment was not completely equilibrated between glyceraldehyde 3-phosphate and dihydroxyacetone phosphate precursor pools ( $U_{\text{calc}} < U_{\text{table}}$ ). In both experiments, C3 and C4 resonances can be resolved into singlet and doublet components, the doublet representing the  $[3,4-^{13}\text{C}_2]$ glucose isotopomer (Fig. 2). After subtraction of the NA contribution from the singlet signal, the ratio between the doublet and the total (singlet and correspondent doublet) provides the enrichment of the triose phosphate

precursor pool (Fig. 1 and Table 1).  $[1-^{13}\text{C}]$ Lactate and  $[^{13}\text{C}]$ bicarbonate substrates enriched the triose phosphate precursor pool to similar levels ( $U_{\text{calc}} < U_{\text{table}}$ ). Also, for both tracers, the  $^{13}\text{C}$  enrichment of glucose was only marginally less than that of the triose phosphate pool, indicating that GNG accounted for almost all hepatic GP. This was an expected result because, after 24 h of fasting, almost all glycogen is depleted.

### Glucose enrichment from $^2\text{H}_2\text{O}$ assessed by $^2\text{H}$ NMR

On conversion to MAG, the  $^2\text{H}$ -NMR signals of glucose are well resolved allowing precise quantification of their relative intensities. These values are directly proportional to the relative  $^2\text{H}$  enrichments in the respective sites of glucose, and the fraction of glucose derived from GNG is equal to the intensity of signal 5 relative to that of signal 2. As shown in Fig. 3, the intensity of signal 5 approached that of H2, indicating that GNG was the principal source of GP:  $100 \pm 1\%$  and  $99 \pm 1\%$  for the perfusion with  $[^{13}\text{C}]$ bicarbonate/ $^2\text{H}_2\text{O}$  and  $[1-^{13}\text{C}]$ lactate/ $^2\text{H}_2\text{O}$ , respectively (Figure 4). These data are consistent with the above considerations on fasting glycogen effects and fractional GNG estimates derived from the  $[^{13}\text{C}]$ bicarbonate and  $[1-^{13}\text{C}]$ lactate isotopomer distribution measurements. Enrichment of both H6 sites was significantly lower than that of H2 ( $U_{\text{calc}} > U_{\text{table}}$ ) as seen by the difference in the two signal intensities: the ratio H6S/H2 is equal to  $44 \pm 2\%$  for  $[1-^{13}\text{C}]$ lactate and  $65 \pm 4\%$  for  $[^{13}\text{C}]$ bicarbonate.

## DISCUSSION

### Glucose enrichment analysis by $^{13}\text{C}$ and $^2\text{H}$ NMR

Several tracer methods exist for quantifying the contribution of GNG to hepatic GP. Determination of enrichment of the immediate precursor by MIDA circumvents many of the traditional limitations of carbon tracer measurements as discussed in the introduction. The  $[^{13}\text{C}]$ bicarbonate tracer is evenly distributed throughout the liver, therefore the observed  $^{13}\text{C}$ -enrichment distribution of glucose represents all hepatic GNG activity involving carboxylation reactions of the Krebs cycle. With sufficient sample mass, the  $^{13}\text{C}$ -NMR method can quantify very low excess  $^{13}\text{C}$ -enrichment levels of  $[3,4-^{13}\text{C}_2]$ glucose (13), the product generated from the GNG condensation of two  $^{13}\text{C}$ -enriched triose phosphate molecules. This capability is an important consideration in the MIDA approach because the enrichment level of  $[3,4-^{13}\text{C}_2]$ glucose cannot exceed the square of the enrichment of the triose phosphate precursor pool.

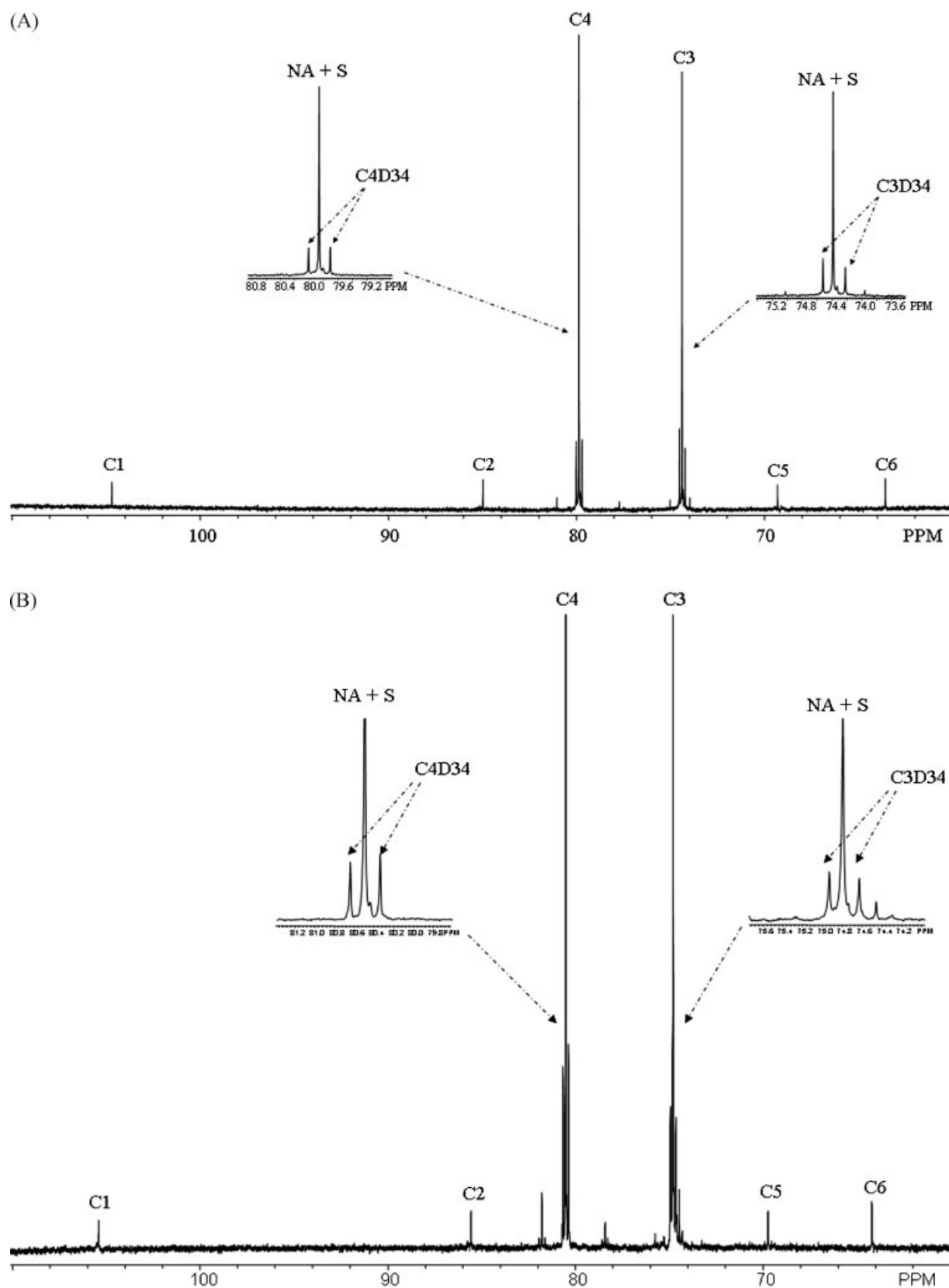


**Figure 2.** Proton-decoupled  $^{13}\text{C}$ -NMR spectrum of MAG derived from perfusate glucose of rats infused with (a)  $[^{13}\text{C}]\text{bicarbonate}/^2\text{H}_2\text{O}$  and (b)  $[1\text{-}^{13}\text{C}]\text{lactate}/^2\text{H}_2\text{O}$ . The six carbons of the glucose skeleton (C1–C6) and an expansion of the signals of C3 and C4 resonances resulting from the incorporation of  $[^{13}\text{C}]\text{bicarbonate}$  are shown. In each expansion, both the singlet (S) and the doublet (C3D34 and C4D34) signals can be resolved.



**Table 1.**  $^{13}\text{C}$  enrichment of glucose measured directly by  $^{13}\text{C}$  NMR, calculated triose phosphate  $^{13}\text{C}$  enrichment by  $^{13}\text{C}$  NMR isotopomer distribution analysis, and the contribution of triose phosphate to GP from the  $[1-^{13}\text{C}]\text{lactate}$  and  $[^{13}\text{C}]\text{bicarbonate}$  perfusion experiments. Values are mean  $\pm$  SE

|          | $[1-^{13}\text{C}]\text{Lactate}$      |                                                 |                                         | $[^{13}\text{C}]\text{Bicarbonate}$    |                                                 |                                         |
|----------|----------------------------------------|-------------------------------------------------|-----------------------------------------|----------------------------------------|-------------------------------------------------|-----------------------------------------|
|          | Glucose $^{13}\text{C}$ enrichment (%) | Triose phosphate $^{13}\text{C}$ enrichment (%) | Triose phosphate contribution to GP (%) | Glucose $^{13}\text{C}$ enrichment (%) | Triose phosphate $^{13}\text{C}$ enrichment (%) | Triose phosphate contribution to GP (%) |
| Carbon 3 | 25 $\pm$ 2                             | 22 $\pm$ 2                                      | 90 $\pm$ 4                              | 21 $\pm$ 1                             | 20 $\pm$ 1                                      | 95 $\pm$ 4                              |
| Carbon 4 | 28 $\pm$ 1                             | 26 $\pm$ 0                                      | 92 $\pm$ 2                              | 19 $\pm$ 1                             | 17 $\pm$ 1                                      | 91 $\pm$ 2                              |

Triose phosphate enrichment from  $[1-^{13}\text{C}]\text{lactate}$  was found to be  $\sim 25\%$ . Given a mixture of 99% 1 mM  $[1-^{13}\text{C}]\text{lactate}$  and 0.1 mM unlabeled pyruvate, the pyruvate pool should be  $\sim 90\%$  enriched. After carboxylation to oxaloacetic acid and randomization of  $^{13}\text{C}$  between C4 and C1, enrichment at each carbon will be reduced by a factor of 2 to  $\sim 45\%$ . Assuming that net anaplerosis is about twice that of the Krebs cycle flux (15), the oxaloacetic acid carboxyls will be further diluted by about two-thirds from the entry of unlabeled carbons derived from acetyl-CoA, resulting in a an enrichment of  $\sim 30\%$ . Recycling of PEP via pyruvate provides additional opportunity for exchange of labeled  $^{13}\text{C}$  with unlabeled  $\text{CO}_2$ , thereby reducing the  $^{13}\text{C}$  enrichment of oxaloacetic acid carboxyls (19). Therefore, the observed triose phosphate enrichment of  $\sim 25\%$  can be explained entirely by exchanges and dilutions at the Krebs cycle level. When these considerations are applied to the  $[^{13}\text{C}]\text{bicarbonate}$  label, we reach a different conclusion. Pyruvate carboxylation and randomization of oxaloacetic acid carbons will reduce the  $^{13}\text{C}$ -labeled precursor enrichment to  $\sim 50\%$ , and dilution from acetyl-CoA will further reduce this to  $\sim 33\%$ . However, in this experiment, PEP recycling will increase the  $^{13}\text{C}$  enrichment of oxaloacetic acid by providing additional opportunity for entry of  $[^{13}\text{C}]\text{bicarbonate}$  via carboxylation. Hence, the triose phosphate enrichment would be expected to be at least 33%, substantially higher than the 20% enrichment that was measured. The most reasonable explanation for this discrepancy is that the  $[^{13}\text{C}]\text{bicarbonate}$  precursor was diluted by exchange with unlabeled  $\text{CO}_2$  from the carbogen gas used to maintain oxygenation and pH of the perfusion fluid.

In the  $^2\text{H}_2\text{O}$  measurement, the ratio of H5/H2 enrichment approached unity, indicating that all GP was from GNG. H6/H2 ratios were significantly less, indicating that there was a substantial contribution of GNG from glycerol, an incomplete exchange between the precursor hydrogens and perfusion water, or most probably an incomplete backward scrambling between malate and fumarate. The H6 pair of glucose are derived from the methylene hydrogens of PEP and oxaloacetic acid and the methyl hydrogens of pyruvate. Unlike H5, which is enriched via the obligatory addition of water hydrogen via enolase or triose phosphate isomerase,  $^2\text{H}$  incorporation into the H6 positions is contingent on exchanges at the level of the Krebs cycle and pyruvate. To the extent that these exchanges are incomplete, glucose H6 enrichment will be less than that of H5.

### Sensitivity and practicality of $^{13}\text{C}$ NMR isotopomer distribution analysis in humans

After overnight fasting, when GNG accounts for  $\sim 50\%$  of GP, a 4% enrichment of the triose phosphate precursor pool would result in a steady-state  $[3,4-^{13}\text{C}_2]\text{glucose}$

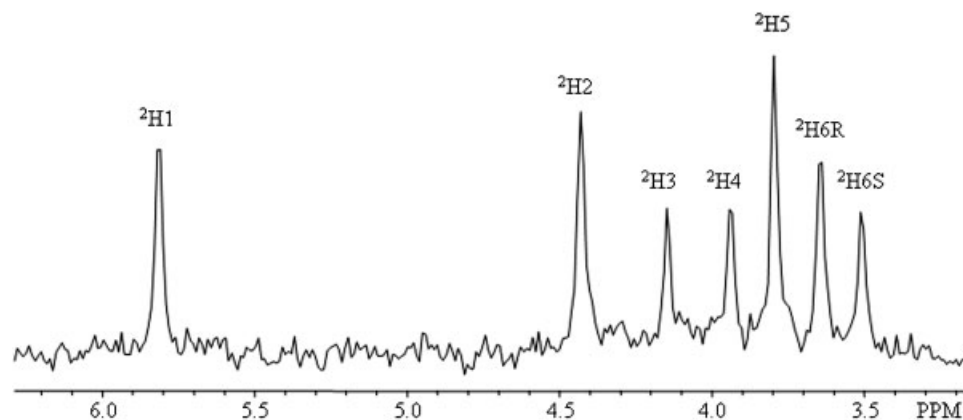


**Figure 3.** Proton-decoupled  $^2\text{H}$ -NMR spectrum of MAG derived from perfusate glucose of rats infused with  $^{13}\text{C}$ -labeled substrates and  $^2\text{H}_2\text{O}$  simultaneously. The deuterium enrichment in each position of the glucose skeleton (from  $^2\text{H}1$  to  $^2\text{H}6$ ) is shown.

abundance of  $\sim 0.16\%$  and excess  $^{13}\text{C}$  enrichment of about 2% in C3 and C4. As demonstrated by Jin *et al.* (13), quantifiable doublet signals from 22  $\mu\text{mol}$  MAG with 0.34% abundance of  $[3,4-^{13}\text{C}_2]\text{glucose}$  were obtained with less than 2 h of NMR collection time. Excess enrichment levels of 2% in C3 and C4 can be precisely quantified if the NA signals of the other carbons have acceptable signal-to-noise ratios. In humans, hepatic Glc6P can be non-invasively sampled by glucuronidation probes such as paracetamol and menthol (10,16), and this approach has two key advantages for quantifying enrichment from GNG tracers compared with the analysis of plasma glucose. First, glucuronides provide higher amounts of analyte ( $>100 \mu\text{mol}$ ) than a 20–30 mL blood collection. Second, the relatively small hepatic sugar phosphate pool sizes ensure that isotopic steady-state from GNG  $^{13}\text{C}$ -labeled precursors is rapidly achieved. We think that the predicted 3,4-hexose  $^{13}\text{C}$ -enrichment levels

of 0.16% should be quantifiable from a urine glucuronide sample with reasonably short collection times (1–2 h) either by direct-detect  $^{13}\text{C}$  NMR or by more sensitive indirect detection methods such as J-resolved heteronuclear single-quantum coherence spectroscopy (17).

Given the dilutions at the Krebs cycle level (6), a 4% enrichment of  $[1-^{13}\text{C}]\text{triose phosphates}$  would require a bicarbonate precursor pool  $^{13}\text{C}$  enrichment of  $\sim 8\%$ . In the study of Allsop *et al.* (18), a steady-state plasma bicarbonate enrichment of  $\sim 0.08\%$  was achieved in 2 h in 75 kg humans by administering a prime of 0.38 mmol sodium  $[^{13}\text{C}]\text{bicarbonate}$  followed by a constant infusion of  $\sim 0.3 \text{ mmol/h}$ . The total amount of sodium  $[^{13}\text{C}]\text{bicarbonate}$  administered was therefore  $\sim 1 \text{ mmol}$ . On this basis, 8%  $^{13}\text{C}$  enrichment of plasma bicarbonate would require about 100 mmol (8.5 g) sodium  $[^{13}\text{C}]\text{bicarbonate}$  tracer. This quantity is comparable to the amounts of  $[1-^{13}\text{C}]\text{acetate}$  or  $[2-^{13}\text{C}]\text{glycerol}$  used in human MIDA studies of lipogenesis and GNG (19,20,21).

In conclusion, we studied the use of  $[^{13}\text{C}]\text{bicarbonate}$  and  $[1-^{13}\text{C}]\text{lactate}$  substrates and a simple  $^{13}\text{C}$  NMR isotopomer analysis for quantification of the fraction of hepatic glucose derived from GNG. The method used to measure GNG was based on the  $^{13}\text{C}$  enrichment of the immediate glucose precursor which overcomes the limitations of the usual methodologies. The results from  $^{13}\text{C}$  and  $^2\text{H}$  analysis were similar, thus validating the method.

### Acknowledgements

This work was supported by grants POCTI/CBO/38611/01, POCTI/QUI/55603/2004 and POCI/SAU-OBS/55802/04 from FCT-MCES.

### REFERENCES

1. Hellerstein MK, Neese RA. Mass isotopomer distribution analysis at eight years: theoretical, analytic, and experimental considerations. *Am. J. Physiol.* 1999; **276**: E1146–1170.

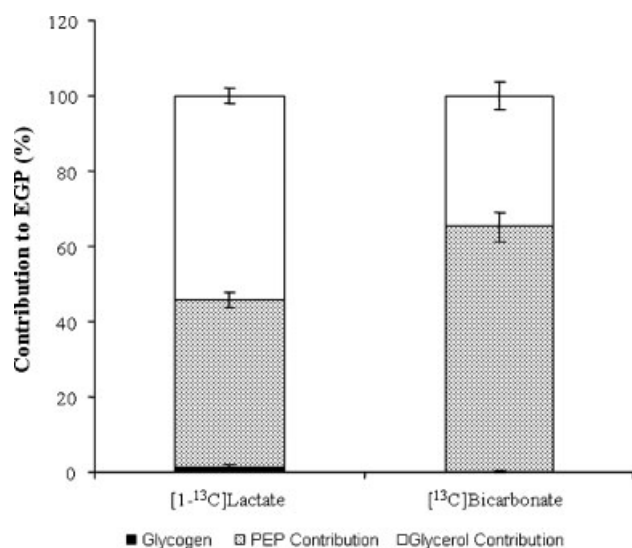


**Figure 4.** Percentage contribution of glycogenolysis (dark bar) and GNG (shaded and white bars) to GP in the two perfusion experiments. GNG is subdivided into contribution of PEP (bar with black dots) and glycerol (white bar).

2. Neese RA, Schwarz JM, Faix D, Turner S, Letscher A, Vu D, Hellerstein MK. Gluconeogenesis and intrahepatic triose phosphate flux in response to fasting or substrate loads. Application of the mass isotopomer distribution analysis technique with testing of assumptions and potential problems. *J. Biol. Chem.* 1995; **270**: 14452–14466.
3. Landau BR, Wahren J, Previs SF, Ekberg K, Chandramouli V, Brunengraber H. Glycerol production and utilization in humans: sites and quantitation. *Am. J. Physiol.* 1996; **271**: E1110–1117.
4. Remesy C, Demigne C. Changes in availability of gluconeogenic and ketogenic substrates and liver metabolism in fed or starved rats. *Ann. Nutr. Metab.* 1983; **27**: 57–70.
5. Previs SF, Hallowell PT, Neimanis KD, David F, Brunengraber H. Limitations of the mass isotopomer distribution analysis of glucose to study gluconeogenesis. Heterogeneity of glucose labeling in incubated hepatocytes. *J. Biol. Chem.* 1998; **273**: 16853–16859.
6. Esenmo E, Chandramouli V, Schumann WC, Kumaran K, Wahren J, Landau BR. Use of  $^{14}\text{CO}_2$  in estimating rates of hepatic gluconeogenesis. *Am. J. Physiol.* 1992; **263**: E36–41.
7. Jones JG, Solomon MA, Cole SM, Sherry AD, Malloy CR. An integrated  $^2\text{H}$  and  $^{13}\text{C}$  NMR study of gluconeogenesis and TCA cycle flux in humans. *Am. J. Physiol. Endocrinol. Metab.* 2001; **281**: E848–856.
8. Jones JG, Perdigoto R, Rodrigues TB, Geraldles CF. Quantitation of absolute  $^2\text{H}$  enrichment of plasma glucose by  $^2\text{H}$  NMR analysis of its monoacetone derivative. *Magn. Reson. Med.* 2002; **48**: 535–539.
9. Perdigoto R, Furtado AL, Porto A, Rodrigues TB, Geraldles CF, Jones JG. Sources of glucose production in cirrhosis by  $^2\text{H}_2\text{O}$  ingestion and  $^2\text{H}$  NMR analysis of plasma glucose. *Biochim. Biophys. Acta* 2003; **1637**: 156–163.
10. Burgess SC, Weis B, Jones JG, Smith E, Merritt ME, Margolis D, Sherry AD, Malloy CR. Noninvasive evaluation of liver metabolism by  $^2\text{H}$  and  $^{13}\text{C}$  NMR isotopomer analysis of human urine. *Anal. Biochem.* 2003; **312**: 228–234.
11. Burgess SC, Hausler N, Merritt M, Jeffrey FM, Storey C, Milde A, Koshy S, Lindner J, Magnuson MA, Malloy CR, Sherry AD. Impaired tricarboxylic acid cycle activity in mouse livers lacking cytosolic phosphoenolpyruvate carboxykinase. *J. Biol. Chem.* 2004; **279**: 48941–48949.
12. Snowden J. Preparation of 1- $^{14}\text{C}$ -D-Xylose from 1- $^{14}\text{C}$ -D-Glucose. *J. Am. Chem. Soc.* 1951; **73**: 5496–5497.
13. Jin ES, Jones JG, Burgess SC, Merritt ME, Sherry AD, Malloy CR. Comparison of [3,4- $^{13}\text{C}_2$ ]glucose to [6,6- $^2\text{H}_2$ ]glucose as a tracer for glucose turnover by nuclear magnetic resonance. *Magn. Reson. Med.* 2005; **53**: 1479–1483.
14. Perdigoto R, Rodrigues TB, Furtado AL, Porto A, Geraldles CF, Jones JG. Integration of [U- $^{13}\text{C}$ ]glucose and  $^2\text{H}_2\text{O}$  for quantification of hepatic glucose production and gluconeogenesis. *NMR Biomed.* 2003; **16**: 189–198.
15. Jones JG, Naidoo R, Sherry AD, Jeffrey FM, Cottam GL, Malloy CR. Measurement of gluconeogenesis and pyruvate recycling in the rat liver: a simple analysis of glucose and glutamate isotopomers during metabolism of [1,2,3- $^{13}\text{C}_3$ ]propionate. *FEBS Lett.* 1997; **412**: 131–137.
16. Ribeiro A, Caldeira MM, Carvalheiro M, Bastos M, Baptista C, Fagulha A, Barros L, Barosa C, Jones JG. Simple measurement of gluconeogenesis by direct  $^2\text{H}$  NMR analysis of menthol glucuronide enrichment from  $^2\text{H}_2\text{O}$ . *Magn. Reson. Med.* 2005; **54**: 429–434.
17. Burgess SC, Carvalho RA, Merritt ME, Jones JG, Malloy CR, Sherry AD.  $^{13}\text{C}$  isotopomer analysis of glutamate by J-resolved heteronuclear single quantum coherence spectroscopy. *Anal. Biochem.* 2001; **289**: 187–195.
18. Allsop JR, Wolfe RR, Burke JF. Tracer priming the bicarbonate pool. *J. Appl. Physiol.* 1978; **45**: 137–139.
19. Neese RA, Faix D, Kletke C, Wu K, Wang AC, Shackleton CH, Hellerstein MK. Measurement of endogenous synthesis of plasma cholesterol in rats and humans using MIDA. *Am. J. Physiol.* 1993; **264**: E136–147.
20. Schwarz JM, Linfoot P, Dare D, Aghajanian K. Hepatic de novo lipogenesis in normoinsulinemic and hyperinsulinemic subjects consuming high-fat, low-carbohydrate and low-fat, high-carbohydrate isoenergetic diets. *Am. J. Clin. Nutr.* 2003; **77**: 43–50.
21. Hellerstein MK, Neese RA, Linfoot P, Christiansen M, Turner S, Letscher A. Hepatic gluconeogenic fluxes and glycogen turnover during fasting in humans. A stable isotope study. *J. Clin. Invest.* 1997; **100**: 1305–1319.